Published in final edited form as:

Nature. 2011 February 3; 470(7332): 115–119. doi:10.1038/nature09671.

Oncogenically active *MYD88* mutations in human lymphoma

Vu N. Ngo[1,†,*], **Ryan M. Young**[1,*], **Roland Schmitz**[1,*], **Sameer Jhavar**[1,*], **Wenming Xiao**[2,*], **Kian-Huat Lim**[1,*], **Holger Kohlhammer**[1], **Weihong Xu**[1], **Yandan Yang**[1], **Hong Zhao**[1], **Arthur L. Shaffer**[1], **Paul Romesser**[1,3], **George Wright**[4], **John Powell**[2], **Andreas Rosenwald**[5], **Hans Konrad Muller-Hermelink**[5], **German Ott**[6], **Randy D. Gascoyne**[7], **Joseph M. Connors**[7], **Lisa M. Rimsza**[8,9], **Elias Campo**[10], **Elaine S. Jaffe**[11], **Jan Delabie**[12], **Erlend B. Smeland**[13], **Richard I. Fisher**[9,14], **Rita M. Braziel**[9,15], **Raymond R. Tubbs**[9,16], **J. R. Cook**[9,16], **Denny D. Weisenburger**[17], **Wing C. Chan**[17], and **Louis M. Staudt**[1]

[1]Metabolism Branch, Center for Cancer Research, National Cancer Institute, NIH, Bethesda, Maryland 20892, USA

[2]Bioinformatics and Molecular Analysis Section, Division of Computational Bioscience, Center for Information Technology, National Institutes of Health, Bethesda, Maryland 20892, USA

[3]Howard Hughes Medical Institute-National Institutes of Health Research Scholars Program, Bethesda, Maryland 20892, USA

[4]Biometric Research Branch, DCTD, National Cancer Institute, NIH, Bethesda, Maryland 20892, USA

[5]Department of Pathology, University of Würzburg, 97080 Würzburg, Germany

[6]Department of Clinical Pathology, Robert-Bosch-Krankenhaus, and Dr Margarete Fischer-Bosch Institute for Clinical Pharmacology, 70376 Stuttgart, Germany

[7]British Columbia Cancer Agency, Vancouver, British Columbia V5Z 4E6, Canada

[8]Department of Pathology, University of Arizona, Tucson, Arizona 85724, USA

[9]Southwest Oncology Group, 24 Frank Lloyd Wright Drive, Ann Arbor, Michigan 48106, USA

[10]Hospital Clinic, University of Barcelona, 08036 Barcelona, Spain

[11]Laboratory of Pathology, Center for Cancer Research, National Cancer Institute, NIH, Bethesda, Maryland 20892, USA

Correspondence and requests for materials should be addressed to L.M.S. (lstaudt@mail.nih.gov).

[†]Present address: Division of Hematopoietic Stem Cell and Leukemia Research, City of Hope National Medical Center, Duarte, California 91010, USA.

[*]These authors contributed equally to this work.

Supplementary Information is linked to the online version of the paper at www.nature.com/nature.

Author Contributions

V.N.N., R.M.Y., R.S., S.J., K.-H.L., H.K. and A.L.S. designed and performed experiments. W.X., Y.Y. and H.Z. performed experiments. W.X., G.W. and J.P. analysed data. A.R., H.K.M.-H., G.O., R.D.G., J.M.C., L.M.R., E.C., E.S.J., J.D., E.B.S., R.I.F., R.M.B., R.R.T., J.R.C., D.D.W. and W.C.C. supplied patient samples and reviewed pathological and clinical data. L.M.S. designed and supervised research and wrote the manuscript.

Gene expression profiling data have been submitted to GEO under accession number GSE22900.

The authors declare no competing financial interests.

[12]Pathology Clinic, Rikshospitalet University Hospital, N-0310 Oslo, Norway

[13]Institute for Cancer Research, Rikshospitalet University Hospital and Center for Cancer Biomedicine, Faculty Division of the Norwegian Radium Hospital, University of Oslo, N-0310 Oslo, Norway

[14]James P. Wilmot Cancer Center, University of Rochester School of Medicine, Rochester, New York 14642, USA

[15]Oregon Health and Science University, Portland, Oregon 97239, USA

[16]Cleveland Clinic Pathology and Laboratory Medicine Institute, Cleveland, Ohio 44195, USA

[17]Departments of Pathology and Microbiology, University of Nebraska Medical Center, Omaha, Nebraska 68198, USA

Abstract

The activated B-cell-like (ABC) subtype of diffuse large B-cell lymphoma (DLBCL) remains the least curable form of this malignancy despite recent advances in therapy[1]. Constitutive nuclear factor (NF)-κB and JAK kinase signalling promotes malignant cell survival in these lymphomas, but the genetic basis for this signalling is incompletely understood. Here we describe the dependence of ABC DLBCLs on MYD88, an adaptor protein that mediates toll and interleukin (IL)-1 receptor signalling[2,3], and the discovery of highly recurrent oncogenic mutations affecting MYD88 in ABC DLBCL tumours. RNA interference screening revealed that MYD88 and the associated kinases IRAK1 and IRAK4 are essential for ABC DLBCL survival. High-throughput RNA resequencing uncovered *MYD88* mutations in ABC DLBCL lines. Notably, 29% of ABC DLBCL tumours harboured the same amino acid substitution, L265P, in the MYD88 Toll/IL-1 receptor (TIR) domain at an evolutionarily invariant residue in its hydrophobic core. This mutation was rare or absent in other DLBCL subtypes and Burkitt's lymphoma, but was observed in 9% of mucosa-associated lymphoid tissue lymphomas. At a lower frequency, additional mutations were observed in the MYD88 TIR domain, occurring in both the ABC and germinal centre B-cell-like (GCB) DLBCL subtypes. Survival of ABC DLBCL cells bearing the L265P mutation was sustained by the mutant but not the wild-type MYD88 isoform, demonstrating that L265P is a gain-of-function driver mutation. The L265P mutant promoted cell survival by spontaneously assembling a protein complex containing IRAK1 and IRAK4, leading to IRAK4 kinase activity, IRAK1 phosphorylation, NF-κB signalling, JAK kinase activation of STAT3, and secretion of IL-6, IL-10 and interferon-β. Hence, theMYD88 signalling pathway is integral to the pathogenesis of ABC DLBCL, supporting the development of inhibitors of IRAK4 kinase and other components of this pathway for the treatment of tumours bearing oncogenic MYD88 mutations.

The current molecular taxonomy of DLBCL distinguishes three main subtypes: ABC, GCB and primary mediastinal B-cell lymphoma (PMBL)[4]. Current therapy is least successful in ABC DLBCL, achieving less than a 40% cure rate[1]. The anti-apoptotic NF-κB signalling pathway is constitutively active in ABC DLBCL owing to oncogenic CARD11 mutations or chronic active B-cell receptor signalling, augmented by inactivation of A20[5–8]. A subset of ABC DLBCLs use JAK kinase signalling to activate the transcription factor STAT3, a

pathway that synergizes with NF-κB in promoting cell survival[9,10]. The oncogenic aetiology of this JAK–STAT3 signalling has not been elucidated.

We conducted an RNA interference (RNAi) screen for genes that are required for proliferation and survival of lymphoma cell lines and identified three small hairpin RNAs (shRNAs) targeting *MYD88* that were toxic to two ABC DLBCL lines but not to two GCB DLBCL lines (Supplementary Fig. 1a). During normal immune responses, MYD88 functions as a signalling adaptor protein that activates the NF-κB pathway after stimulation of toll-like receptors (TLRs) and receptors for IL-1 and IL-18 (refs 2, 3). MYD88 coordinates the assembly of a multi-subunit signalling complex consisting of various members of the IRAK family of serine-threonine kinases[11]. The initial RNAi screen also identified two shRNAs targeting *IRAK1* as toxic for one or both of the ABC DLBCL lines, but not for GCB DLBCL lines. A subsequent screen identified additional *MYD88* and *IRAK1* shRNAs that were toxic to all five ABC DLBCL lines tested but had little effect on GCB DLBCL, Burkitt's lymphoma, mantle cell lymphoma and multiple myeloma lines (Supplementary Fig. 1a). Using shRNAs targeting the 3′ untranslated regions of *MYD88* and *IRAK1*, which reduced expression of their respective proteins (Supplementary Fig. 1c), we showed that ABC DLBCL cells could be rescued from shRNA-mediated toxicity by coexpression of coding region cDNAs (*IRAK1*, Supplementary Fig. 1d; *MYD88*, see below). *MYD88* and *IRAK1* shRNAs displayed a time-dependent toxicity for ABC DLBCL lines and induced apoptosis, but had little effect on GCB DLBCL and myeloma lines (Fig. 1 and Supplementary Fig. 1b, e). Together these data establish that MYD88 and IRAK1 are required to maintain the viability of ABC DLBCL cells.

To comprehensively discover somatic mutations in ABC DLBCL, we used high-throughput resequencing of mRNA to search for sequence variants in four ABC DLBCL lines. In addition to known mutations in *CARD11* and *CD79B*, we identified a single nucleotide variant that changed a leucine residue at position 265 of the *MYD88* coding region to proline (L265P) in all four ABC DLBCL lines tested. This variant resides in the MYD88 TIR domain, which interacts with TIR domains of various receptors during innate immune responses and also mediates homotypic interactions[12,13].

To extend this finding, we resequenced the *MYD88* coding region in 382 lymphoma biopsy samples. The L265P mutation was by far the most common variant observed, occurring in 29% of ABC DLBCL biopsies. By contrast, this mutation was rare or absent among DLBCLs of the GCB and PMBL subtypes and among Burkitt's lymphomas (Fig. 2b). Of note, *MYD88* L265P was also observed in 9% of gastric mucosa-associated lymphoid tissue (MALT) lymphomas. Most *MYD88* L265P mutations appeared heterozygous by sequencing, but six biopsy samples and one ABC DLBCL line (OCI-Ly3) were homozygous. By array-based comparative genomic hybridization[14], 56% (15 of 27) of the ABC DLBCL cases with gain or amplification of the *MYD88* locus had the L265P mutation, compared to 29% (13 of 45) with wild-type *MYD88* copy number ($P = 0.023$), indicating selection by the cancer cells for this mutant allele. A host of other, less common *MYD88* mutations were equally distributed among ABC and GCB DLBCL cases (Fig. 2a, b). Whereas most mutations were in the TIR domain, one mutation (V52M) was in the death domain and two were between the death and TIR domains (S149G/I). Six ABC DLBCL

lines had a *MYD88* mutation (Fig. 1), whereas all 14 GCB DLBCL lines tested were wild type. In 13 DLBCL cases for which matched germline DNA was available, the *MYD88* mutations (L265P, V217F, S219C, M232T, S243N, T294P) were confirmed to be somatically acquired. Overall, *MYD88* mutations were observed in 39% of ABC DLBCLs (Fig. 2b), establishing *MYD88* as among the most frequently altered genes in this malignancy.

The *MYD88* mutations partially overlapped with abnormalities in *CD79B/A, A20* and *CARD11* in ABC DLBCL tumours (Fig. 2c). Among cases with a *MYD88* L265P mutation, 34% had a coincident CD79B/A mutation whereas this overlap was significantly less common among ABC DLBCLs without a CD79B/A mutation (18%; $P = 0.03$). These data raise the possibility of a functional interaction between the chronic active B-cell receptor signalling that is associated with CD79B/A mutations[8] and the signalling that is instigated by the *MYD88* L265P mutation. Some cases had *MYD88* L265P as well as a *CARD11* mutation, which strongly activates NF-κB, suggesting that the *MYD88* mutation confers additional biological attributes beyond NF-κB activation.

The location of the *MYD88* mutations within the three-dimensional structure of the MYD88 TIR domain was both surprising and instructive (Fig. 2d). The L265P mutation occurs at a residue that is invariant in evolution and contributes to a β-sheet at the hydrophobic core of the domain. Another mutation, M232T, affects a methionine that is in an adjacent β-sheet and contacts the leucine affected by L265P. A cluster of mutations were in the 'B–B loop', an evolutionarily conserved region that mediates TIR domain interactions[15]. Two other mutations, S222R and S243N, alter an adjoining face of the TIR domain. Only one mutant affects the opposite side of the TIR domain (T294P), altering the conserved 'box 3' motif that is important in IL-1 signalling[13].

To examine whether the *MYD88* mutants confer a gain or loss of function, we performed a complementation experiment in which we knocked down endogenous *MYD88* in ABC DLBCL lines and ectopically expressed wild-type or mutant *MYD88* coding regions. In ABC DLBCL lines harbouring an L265P mutation, *MYD88* L265P rescued the cells after *MYD88* knockdown, but wild-type *MYD88* was ineffective (Fig. 2e), although these *MYD88* isoforms were expressed equivalently (data not shown). Hence, these ABC DLBCLs are 'addicted' to the action of the L265P MYD88 mutant, indicating that it is a gain-of-function driver mutation that confers a selective advantage during the evolution of ABC DLBCL tumours.

To assess the biochemical and functional consequences of the *MYD88* mutations, we fused green fluorescent protein (GFP) to MYD88 and introduced the fusion proteins into DLBCL lines. Immunoprecipitation of MYD88–GFP with anti-GFP antibodies brought down IRAK1 and IRAK4, two kinases known to associate with MYD88 upon TLR or IL-1 stimulation (Fig. 3a)[3]. During IL-1 signalling, IRAK1 becomes hyperphosphorylated by IRAK4, resulting in slowly migrating IRAK1 isoforms[16]. In cells bearing the MYD88 L265P, a prominent, slow-migrating IRAK1 species co-immunoprecipitated with MYD88 (Fig. 3a). By contrast, wild-type MYD88 did not associate strongly with these IRAK1 isoforms nor did the other MYD88 mutants tested (Fig. 3b). Treatment with λ-phosphatase collapsed the

slow-migrating IRAK1 species into a single band, confirming that they are phosphorylated IRAK1 isoforms (Fig. 3c). Phosphorylation of endogenous IRAK1 was observed in an ABC DLBCL line with L265P but not in a GCB DLBCL line (Fig. 3c). Thus, the MYD88 L265P mutant nucleates a signalling complex in ABC DLBCLs that includes phosphorylated IRAK1, consistent with a gain-of-function phenotype.

IRAK4 co-immunoprecipitated with MYD88, but it associated equivalently with wild-type and L265P MYD88 (Fig. 3a). Knockdown of IRAK4 was toxic for ABC DLBCL lines but not for GCB DLBCL and myeloma lines (Fig. 3d and Supplementary Fig. 1c). Wild-type IRAK4 rescued ABC DLBCL lines after *IRAK4* shRNA induction, but a kinase-dead IRAK4 isoform could not (Fig. 3e), despite equivalent expression (data not shown). By contrast, IRAK1 kinase activity was not required for the survival of ABC DLBCL cells (Supplementary Fig. 1d). A selective small-molecule inhibitor of IRAK1 and IRAK4 kinase activity[17] killed ABC DLBCL lines but not GCB DLBCL and myeloma lines (Fig. 3f). Together, these findings demonstrate that ABC DLBCLs rely upon IRAK4 kinase activity to transduce signals from MYD88 L265P that promote survival.

To investigate signalling pathways that are engaged by MYD88 L265P, we knocked it down in an ABC DLBCL line and profiled the ensuing gene expression changes (Supplementary Table 1 and Supplementary Fig. 2). We identified 285 genes that were down-modulated after *MYD88* knockdown, and searched for overlap between this MDY88 signature and previously defined gene expression signatures[18] (Supplementary Table 2). The most significantly enriched signature reflects NF-κB signalling in ABC DLBCL (44× enrichment, $P = 2.4 \times 10^{-130}$). This signature was also inhibited after *IRAK1* knockdown (Supplementary Fig. 3), indicating that IRAK1 mediates NF-κB activation by MYD88 L265P. To compare the ability of wild-type and mutant MYD88 isoforms to activate NF-κB, we expressed them as GFP fusion proteins in a GCB DLBCL line with little endogenous NF-κB activity. Whereas wild-type MYD88 activated an NF-κB-dependent reporter modestly, L265P had strong activity, as did M232T and S243N, whereas S222R and T294P had an intermediate effect (Fig. 4b). At all MYD88 expression levels, L265P was superior to wild-type MYD88 in upregulating CD83, a previously established NF-κB target in this system[5] (Fig. 4c). Other MYD88 mutants induced CD83 to varying degrees but all were more active than wild-type MYD88. Thus, mutant MYD88 isoforms can contribute to the constitutive NF-κB activation that typifies ABC DLBCL[19].

A signature of JAK kinase signalling in ABC DLBCL overlapped significantly with the MYD88 signature (Fig. 4a; 14× enrichment, $P = 9.6 \times 10^{-39}$) and with IRAK1-regulated genes (Supplementary Fig. 3b). This was notable because autocrine secretion of IL-6 and IL-10 drives JAK–STAT3 signalling in a subset of ABC DLBCLs[9]. *MYD88* knockdown significantly diminished the secretion of IL-6 and IL-10 as well as the phosphorylation of STAT3 in several ABC DLBCL lines (Fig. 4d, e and Supplementary Fig. 1f). IL-6 and IL-10 secretion was also blocked by the IRAK1/4 kinase inhibitor, indicating that IRAK4 links MYD88 L265 signalling to the expression of these cytokines (Fig. 3g). Previous work identified a 'STAT3–high' subgroup of ABC DLBCL tumours with autocrine IL-6/IL-10 signalling and STAT3 phosphorylation, which was missing in a 'STAT3-low' subgroup[9]. The *MYD88* L265P mutation was significantly more common in the STAT3-high subgroup

(37%) than in the STAT3-low subgroup (13%) ($P = 0.0036$), and other *MYD88* mutations were modestly enriched among STAT3-high cases as well (Fig. 4f). These data indicate that *MYD88* mutations contribute to JAK–STAT3 signalling in ABC DLBCL tumours.

The MYD88 signature included a number of genes that are induced by type I interferon (Fig. 4a; 7× enrichment, $P = 4.3 \times 10^{-10}$), which is intriguing given that MYD88 signalling can induce interferon (IFN)-β production by innate immune cells. IFN-β was measurable in the supernatant of the OCI-Ly3 ABC DLBCL line, and *MYD88* knockdown diminished its secretion (Fig. 4d). *MYD88* knockdown decreased IFN-β mRNA levels in the HBL1 line (Supplementary Fig. 2), although IFN-β secretion was below the detection limit. Future work should address whether the secretion of immunomodulatory cytokines such as IFN-β, IL-6 and IL-10 influences immune cells in the microenvironment of ABC DLBCL tumours.

Given the pleiotropic action of MYD88 L265P, we investigated whether MYD88 signalling cooperates with B-cell receptor signalling to maintain ABC DLBCL survival. Knockdown of *MYD88* enhanced the killing of an ABC DLBCL line with chronic active BCR signalling by *CD79B* or *CARD11* shRNAs (Fig. 4g). This finding indicates that MYD88 and B-cell receptor signalling provide non-redundant survival signals to ABC DLBCL cells, in keeping with the fact that some ABC DLBCL tumours harbour *MYD88* L265P as well as *CD79B* or *CARD11* mutations (Fig. 2c).

Our genetic and functional data establish a new oncogenic pathway in lymphomagenesis. Somatically acquired *MYD88* mutations in ABC DLBCL promote NF-κB and JAK–STAT3 signalling, which mediate cell survival in this lymphoma type[9,19]. MYD88 L265P was the most biologically potent mutant and was unique in its ability to coordinate a stable signalling complex containing phosphorylated IRAK1, which probably accounts for its high recurrence among lymphomas. MYD88 L265P also genetically links MALT lymphoma with ABC DLBCL, two lymphoma subtypes that share other oncogenic features[7,14,20–22]. Other *MYD88* mutations may also be drivers of lymphomagenesis given their recurrent nature and ability to activate NF-κB. From a therapeutic standpoint, the signalling complex coordinated by MYD88 L265P represents an enticing target. Our study also provides a genetic method to identify patients whose tumours may depend upon MYD88 signalling and who may therefore benefit from therapies targeting IRAK4 alone or in combination with agents targeting the B-cell receptor[8], NF-κB[23,24] or JAK–STAT3 pathways[9].

METHODS

Cell lines

Cell lines were cultured in RPMI 1640 medium supplemented with penicillin/streptomycin and 10% fetal bovine serum or, for the OCI series of cell lines, Iscove's medium with 20% fresh human plasma. Cells were maintained in a humidified, 5%CO_2 incubator at 37 °C. All cell lines were engineered to express an ecotropic retroviral receptor and the bacterial tetracycline repressor as previously described[25].

Retroviral vectors and retroviral transduction

A previously described retroviral vector, pRSMX[25], was used to express shRNA for the library screen. A modified version of this vector, pRSMX-PG, in which the puromycin selectable marker was fused with the green fluorescence protein (GFP), was used to co-express shRNA and GFP for shRNA toxicity assay. Retroviral transduction was performed by transfecting the retroviral vector and a mixture of helper plasmids for a mutant ecotropic envelope and *gag* and *pol* into 293T cells using Lipofectamine 2000 (Invitrogen). Retroviral supernatants were harvested 48 h after transfection and were used to transduce ecotropic receptor-expressing target cells by centrifugation at 2,500 r.p.m. for 1.5 h in the presence of 8 μg ml^{-1} polybrene.

shRNA library screening

Pools of shRNA library were screened as previously described[25]. Briefly, pools of roughly 1,000 shRNA expressing retroviral vectors were used to transduce target cell lines. After puromycin selection, stable integrants were induced to express shRNA by doxycycline (20 ng ml^{-1}). Parallel uninduced cultures were kept as control. After 3 weeks of shRNA induction, genomic DNA from both uninduced and induced cultures were harvested. shRNA-associated bar code sequences from the genomic DNA were PCR amplified and *in vitro* transcribed, as described[25]. The transcribed RNA products were labelled fluorescently with either Cy5 (induced) or Cy3 (uninduced) using the Universal Linkage System (Amersham Biosciences) and hybridized onto microarrays containing DNA oligonucleotides complementary to the bar code sequences, as described[25]. Each bar code experiment was performed in quadruplicate, and the microarray results for each bar code were averaged. The complete screening results are presented in Supplementary Table 3, which includes some data that have been previously published[8,25].

shRNA sequences

The shRNA sequences used in individual experiments are listed in Supplementary Table 4.

shRNA toxicity and complementation assays

shRNA toxicity was assayed as described[25]. Briefly, the pRSMX-PG vector that co-expresses shRNA and GFP was transduced into lymphoma and multiple myeloma cell lines. Two days after retroviral transduction, doxycycline was added to induce shRNA expression. The fraction of GFP^+, shRNA-expressing cells relative to the GFP^-, $shRNA^-$ fraction was monitored over various time points by flow cytometry and plotted against the same GFP^+, shRNA-expressing fraction on day 0 of doxycycline induction. The reduction of the GFP^+, shRNA-expressing fraction at later time points indicates shRNA toxicity. Complementation studies were performed in the DLBCL cell line that harbours the MYD88 L265P mutation. HBL1 cells were transduced with retroviral vectors that co-express GFP and shRNA targeting the 3′ UTR of *MYD88* (or *IRAK1*). shRNA-transduced cells were subsequently infected with retroviruses co-expressing wild-type or mutant MYD88 (or IRAK1) coding regions and mouse CD8 (Lyt2). The cell fraction positive for GFP and CD8 (using anti-mouse CD8a, BD Pharmingen) was monitored over time by flow cytometry as above. TMD8 and OCI-Ly3 cells were first transduced with retroviruses co-expressing wild-type or mutant

MYD88 (or IRAK1) coding regions and mouse CD8 (Lyt2) and enriched for Lyt2 expression with magnetic beads. Enriched cells were subsequently infected with retroviral vectors that co-express GFP and an shRNA targeting the 3′ UTR of *MYD88*. The cell fraction positive for GFP and CD8 was monitored over time by flow cytometry.

For the IRAK4 complementation assay, HBL1, HLY1, TMD8 and SUDHL2 lymphoma cell lines were first retrovirally transduced with either vLyt2 empty vector, or vLyt2 vector expressing wild-type or kinase-dead IRAK4 (K213A/K214A). The infected cells were later enriched using the CD8 microbeads method (Miltenyi Biotec) according to manufacturer's protocol. The enriched cells were then infected with retroviral vector pRSMX-PG expressing either a control shRNA or an *IRAK4* shRNA. Doxycycline was added 2 days after infection to induce shRNA expression. The fraction of GFP-positive cells was monitored over time by FACS analysis and the decline of GFP hence shRNA expressing cells indicates toxicity.

Synergistic toxicity of MYD88 and either CARD11 or CD79A knockdown

OCI-Ly10 cells were first infected with either pRSMX-puro empty vector or pRSMX-puro vector encoding *MYD88* shRNA sequence (5′-GTACCAGTATTTATACCTCTA-3′). Two days after infection the two cells lines were selected using 1 μg ml^{-1} puromycin. The selected cells were then retrovirally infected with pRSMX-PG encoding either a scramble control, shRNA sequence against *CARD11* (target sequence 5′-GGGGTGTGTACCAGGCTATGA-3′) or *CD79A* (target sequence 5′-GGGGCTTCCTTAGTCATATTC-3′). Doxycycline was added 2 days after infection to induce shRNA expression. The fraction of GFP-positive cells was monitored over time by FACS analysis and the decline of GFP hence shRNA expressing cells indicates toxicity.

High-throughput RNA sequencing/PCR amplification/Sanger sequencing

The standard Illumina pipeline for RNA-seq was used, using paired-end 75-base-pair runs with each sample run in one sequencing lane, yielding ~20 million reads per sample. Sequences were mapped back to both RefSeq and Ensemble transcript models using the BWA algorithm[26], yielding a median resequencing coverage of 10×. Single nucleotide variants (SNVs) were reported that deviated from the human reference genome sequence, were observed in both sequencing directions, represented >20% of the resequencing coverage at a particular base pair position, and were not known SNPs in the dbSNP database of NCBI. A total of 52,160 putative SNVs was detected in the four ABC DLBCL cell lines studied. Sequences have been submitted to the NCBI short sequence archive under accession SRP003192. On the basis of the criteria above, all SNVs that are not represented in publically available databases of single nucleotide polymorphisms (SNPs) are listed in Supplementary Table 5. Except for the MYD88 mutations, other SNVs in this table have not been validated by independent means.

Sanger sequencing of MYD88 was accomplished with the following primers: MYD88-Full-F, 5′-GACCTCTCCAGATCTCAAAAGGCAGATTCC-3′ (PCR amplification and sequencing, exon 1); MYD88-Full-R, 5′-GCAGAAGTACATGGACAGGCAGACAGATAC-3′ (PCR amplification and sequencing,

exon 5); MYD88-Seq-E1R, 5′-TCTCTCCATGGGAGACAGGATGCTG-3′ (sequencing exon 1); MYD88-Seq-E2F, 5′-TGGGTAAAGAGGTAGGCACTCCCAG-3′ (sequencing exon 2); MYD88-Seq-E2R, 5′-GCCCATCTGCTTCAAACACCCATGC-3′ (sequencing exon 2); MYD88-Seq-E3F, 5′-AAGCCTTCCCATGGAGCTCTGACCAC-3′ (sequencing exon 3); MYD88-Seq-E3R, 5′-GCTAGGAGGAGATGCCCAGTATCTG-3′ (sequencing exon 3); MYD88-Seq-E4F, 5′-ACTAAGTTGCCACAGGACCTGCAGC-3′ (sequencing exon 4); MYD88-Seq-E4R, 5′-ATCCAGAGGCCCCACCTACACATTC-3′ (sequencing exon 4); MYD88-Seq-E5F, 5′-GTTGTTAACCCTGGGGTTGAAG-3′ (sequencing exon 5).

For 155 cases of ABC DLBCL, analysis of CARD11, CD79B, and A20 by Sanger sequencing was performed as described[5,8,27].

A20 was declared epigenetically silenced if the expression level in a case was more than 2 standard deviations below the mean of other ABC DLBCL cases, based on previous gene expression profiling data[1]. Deletion of the A20 locus (*TNFAIP3*) was analysed by quantitative PCR using primers to amplify exon 3 and exon 6, as described[27], and compared to a reference gene, *CHMP4A*, that is not subject to copy number alterations in ABC DLBCL. A20 was declared deleted if one or both of the A20 PCR products had an estimated copy number that was more than 3 standard deviations below the average of 9 normal control DNA samples. The following quantitative PCR primers were used: CHMP4A-F, 5′-CTGCAAGGGAGGAGGGGTTTCATTC-3′ (qPCR control gene); CHMP4A-R, 5′-CTTGGGTGTTCCTTCTGGCCAGTC-3′ (qPCR control gene); A20-E3F, 5′-ACCTTTGCTGGGTCTTACATGCAG-3′ (qPCR A20); A20-E3R, 5′-TATGCCCACCATGGAGCTCTGTTAG-3′ (qPCR A20); A20-E6F, 5′-TGAGATCTACTTACCTATGGCCTTG-3′ (qPCR A20); A20-E6R, 5′-TCAGGTGGCTGAGGTTAAAGACAG-3′ (qPCR A20).

Expression vectors and cDNA mutagenesis

The expression vector, vLyt2-MYD88-EGFP, encoding carboxy terminus EGFP-tagged MYD88 was constructed by three-way ligation of PCR-generated MYD88 and EGFP products into the pBMN-IRES-Lyt2 vector (provided by G. Nolan). The restriction site SalI was included in the MYD88 PCR reverse primer and the EGFP PCR forward primer to facilitate the ligation between MYD88 and EGFP. MYD88 or EGFP PCR products were generated using the following primer pairs: 5′-TAGTAGGGATCCGCCGCCACCATGCGACCCGACCGCGCTGA-3′ (MYD88), 5′-TAGTAGGTCGACGGGCAGGGACAAGGCCTTGGC-3′ (MYD88), 5′-TAGTAGGTCGACATGGTGAGCAAGGGCGAGGAG-3′ (EGFP), 5′-TAGTAGGCGGCCGCTTACTTGTACAGCTCGTCCAT-3′ (EGFP).

The expression vector vLyt2-AU1-MYD88 encoding amino terminus AU1-tagged MYD88 was constructed by inserting PCR-generated MYD88 into the pBMN-IRES-Lyt2 vector. MYD88 PCR product was generated using the following primers: 5′-TAGTAGGGATCCGCCGCCACCATGGACACATACCGCTACATCCGACCCGACCGCG CTGAGGCT-3′ and 5′-TAGTAGGCGGCCGCTCAGGGCAGGGACAAGGCCTTGGC-3′.

IRAK1 expression vectors were similarly created by inserting PCR-generated *IRAK1* cDNAs (from pIND-IRAK1 wild type and K239A kinase-dead templates, a gift from X. Li) into the pBMN-IRES-Lyt2 vector, using the following PCR primers: 5′-TAGTAGCTCGAGGCCGCCACCATGGCCGGGGGGCCGGGC-3′ and 5′-TAGTAGGCGGCCGCTCACTTGTCATCGTCGTCCTTGTAGTCGCTCTGAAATTCATCACTTTC-3′.

IRAK4 expression vectors were generated by inserting PCR-generated *IRAK4* cDNA (from a template obtained from the Dana-Farber/Harvard Cancer Center DNA Resource Core) into the pBMN-IRES-Lyt2 vector, using the following primers: 5′-TAGTAGGGATGGGCCGCCACCATGGACACATACCGCTACATCAACAAACCCATAACACCATCA-3′ and 5′-TAGTAGGCGGCCGCTCAAGAAGCTGTCATCTCTTGCAG-3′.

MYD88 mutants were created with the Phusion site-directed mutagenesis kit (New England BioLabs), using either vLyt2-MYD88-EGFP or vLyt2-AU1-MYD88 vector as templates. All cDNA inserts from PCR cloning and site-directed mutagenesis were verified by sequencing. The MYD88 mutagenesis primers used were the following: L265P forward P-CATCAGAAGCGACCGATCCCCATCAAG and L265P reverse P-GGCACCTGGAGAGAGGCTGAGTGCAAA; M232T forward P-AGGTGCCGCCGGACGGTGGTGGTTGTC and M232T reverse P-CTTTTCGATGAGCTCACTAGCAATAGA; S243N forward P-GATTACCTGCAGAACAAGGAATGTGAC and S243N reverse P-ATCAGAGACAACCACCACCATCCGG; T294P forward P-ACCAACCCCTGCCCCAAATCTTGGTTC and T294P reverse P-GTAGTCGCAGACAGTGATGAACCTCAG; S222R forward P-GGTCTATTGCTAGGGAGCTCATCGAAA and S222R reverse P-AGACACAGGTGCCAGGCAGGACATCGC.

The IRAK4 kinase-dead mutant was generated similarly using the following mutagenesis primers: K213A/K214A forward P-ACTGTGGCAGTGGCGGCGCTTGCAGCAATG and K213A/K214A reverse P-TGTGTTATTTACGTAGCCTTTATATACA.

MYD88 co-immunoprecipitation

BJAB cells were retrovirally transduced with various MYD88–GFP fusion constructs co-expressing a Lyt2 surface marker. Cells were enriched for Lyt2 expression using anti-Lyt2 magnetic beads (Invitrogen, 114.47D) following the manufacturer's instructions. Enriched cells were lysed at 10^7 cells per ml in RIPA buffer (0.5% Triton X-100, 0.5% deoxycholate, 0.05% SDS, 10 mM Tris, pH 8.0, 50 mM NaCl, 10 mM EDTA, 1 mM Na_3VO_4, 30 mM pyrophosphate, 10 mM glycerophosphate, 1 mM AEBSF, 0.02 U ml^{-1} aprotinin and 0.01% NaN_3) for 10 min on ice. Lysates were cleared by centrifuging for 20 min at 14,000*g* at 4 °C. MYD88–GFP constructs were immunoprecipitated with washed anti-GFP agarose beads (Chromotek) for 30 min at 4 °C, then washed 3–4 times in 1× RIPA buffer. For λ-phosphatase treatment, the agarose beads were washed two additional times in 10 mM Tris, pH 8.0 with 50 mM NaCl to remove EDTA and phosphates inhibitors. λ-phosphatase (New England Biolabs) treatment was done according to the manufacturer's instructions. Reactions were quenched by the addition of 2× lamellae sample buffer followed by boiling.

Samples were separated on 10% polyacrylamide gels and transferred to Immobilon-p PVDF membranes (Millipore) for western blot analysis. Antibodies used for immunoblotting were anti-IRAK1 rabbit polyclonal (Santa Cruz Biotech), anti-IRAK4 rabbit polyclonal (Cell Signaling Technologies) and anti-MYD88 rabbit monoclonal (Cell Signaling Technologies).

NF-κB reporter assay

BJAB cells retrovirally expressing MYD88–GFP constructs (see above) were transduced with lentiviral particles containing a NF-κB firefly luciferase reporter construct by following the manufacturer's instructions (SA Biosciences). Firefly luciferase activity was measured using the Dual-Luciferase Reporter Assay System (Promega) following the manufacturer's instructions. Luminescence from equivalent amounts of lysate was read in triplicate on a Microtiter Plate Luminometer (Dyn-Ex Technologies). All readings were normalized to the mean fluorescence intensity of MYD88–GFP expression for each MYD88 mutant as determined by FACS analysis on a FACScalibur flow cytometer (Becton Dickinson).

Western blotting

Cells were lysed in lysis buffer (50 mM Tris pH 7.4, 150 mM NaCl, 1% Triton X-100, 1% NP-40, 2 mM EDTA) supplemented with Complete Protease Inhibitor Cocktail Tablets (Roche) and phosphatase inhibitors (Sigma) for 30 min. Lysates were cleared by centrifugation at 15,000*g* at 4 °C for 10 min and protein concentrations were determined by BCA protein assay (Pierce). 80–100 μg of lysates were subjected to electrophoresis through a 4–12% Bis-Tris gel (Invitrogen) and immobilized on the nitrocellulose membranes. Proteins were detected using the following antibodies: MYD88, IRAK4, β-actin, STAT3 and p-STAT3 (Y705) (Cell Signaling Technology).

IRAK1 immunoprecipitation

Cells were lysed at 10^7 cells per ml in RIPA buffer as described above. Lysates were pre-cleared with protein-A agarose beads (Pierce) before incubation with 1 μg ml^{-1} of anti-IRAK1 polyclonal antibody (Santa Cruz Biotech, H-273) for 2 h on ice. Protein-A agarose beads were added to lysates and rotated for 1 h at 4 °C, then washed three times with 1× RIPA buffer. λ-phosphatase treatment was performed as described above. Samples were separated on 10% polyacrylamide gels and transferred to Immobilon-p PVDF membranes (Millipore) for western blot analysis.

Cytokine measurement

The culture medium of cells transduced with inducible shRNAs was replaced with fresh medium plus doxycycline, and the concentrations of IL-6, IL-10 or IFN-β in culture supernatants at the indicated times were measured by ELISA (R&D Systems). Alternatively, unmanipulated lymphoma cells lines were placed into fresh media with the addition of the IRAK1/4 inhibitor (EMD chemicals) and assessed for cytokines as above. The results were normalized to live cell numbers, and are representative of at least two independent experiments.

Apoptosis measurements

HBL1 cells were retrovirally transduced with either control or MYD88-specific shRNAs, as described above. shRNA expression was induced with doxycline and cells were evaluated for apoptosis on 2, 3 and 4 days after induction. To measure apoptosis, cells were first fixed for 10 min with 1.5% paraformaldehyde, centrifuged and then fixed and permeabilized in cold methanol overnight. Methanol-fixed cells were washed three times with FACS buffer (PBS with 1% FBS) and stained with PE rabbit anti-active caspase 3 (BD Pharmingen) and Alexa Fluor 647 mouse anti-cleaved PARP (Asp 214) (BD Pharmingen) for 20 min at room temperature in the dark, followed by an additional wash with FACS buffer. Stained cells were subjected to FACS analysis (FACScalibur, BD) and apoptotic cells were defined as double positive for both active caspase 3 and cleaved PARP.

Cell viability assay by MTS

The described DLBCL and multiple myeloma cells lines were plated in duplicate at a density of 50,000 cells per well in 96-well plates along with DMSO as negative control, or different concentrations of IRAK1/4 inhibitor (EMD Chemicals). Cell viability at 1, 2 and 3 days after drug treatment was assayed by adding 3-(4,5-dimethylthiazol-2-yl)-5-(3-carboxymethoxyphenyl)-2-(4-sulphophenyl)-2H-tetrazolium and an electron coupling reagent (phenazine methosulphate; Promega), incubated for 3 h and measured by the amount of 490 nm absorbance using a 96-well plate reader. The presented data were derived from 3 days of drug treatment. The assay was performed twice.

MYD88 and IRAK1 signature analysis

To generate a gene expression signature of MYD88 signalling in ABC DLBCL, the HBL1 cell line was transduced with retroviral vectors expressing either shMYD88-4 or shMYD88-7. After puromycin selection, shRNA expression was induced for 24 or 48 h and gene expression was measured relative to parallel uninduced cultures using Agilent 4×44K oligonucleotide microarrays. A set of 284 MYD88 target genes was selected as those that were downregulated by 0.4 $\log_2$ in ≥3 arrays. A signature of NF-κB signalling (NF-κB-10 signature; http://lymphochip.nih.gov/signaturedb/) in ABC DLBCL was generated by treating HBL1 cells with the IκB kinase-β inhibitor MLN120B for 2 h, 3 h, 4 h, 6 h, 8 h, 12 h, 16 h and 24 h. Genes that were downregulated >0.4 $\log_2$ in at least four arrays with a one-sided *t*-test <0.01 were chosen. A signature of JAK signalling in ABC DLBCL (JAKUp-2 signature; http://lymphochip.nih.gov/signaturedb/) was generated by treating HBL1 cells with JAK inhibitor I (5 μM; Calbiochem) for 2 h, 4 h, 6 h and 8 h. Genes were chosen that were decreased in expression by >0.4 $\log_2$ at ≥3 time points. A signature of IFN signalling (IFN-3; http://lymphochip.nih.gov/signaturedb/) was curated as the union between three published gene expression signatures of type I interferon signalling (IFN-1, IRF3-1 and Module-3.1 signatures; http://lymphochip.nih.gov/signaturedb/). A Fisher's exact test was used to calculate the significance of the overlap between the MYD88 signature and the other signatures.

Similar methods were used to generate a signature of IRAK1 signalling in ABC DLBCL. Two ABC DLBCL cell lines, HBL1 and TMD8, were transduced with retroviruses expressing shIRAK1-3 or a control shRNA. After puromycin selection, shRNA expression

was induced for 24 h or 48 h and RNA and relative gene expression in shIRAK1 and control shRNA-expressing cells was analysed by gene expression profiling as above. A signature of 350 genes was selected as those that were downregulated by 0.4 $\log_2$ in ≥3 arrays.

Supplementary Material

Refer to Web version on PubMed Central for supplementary material.

Acknowledgments

This research was supported by the Intramural Research Program of the NIH, National Cancer Institute, Center for Cancer Research, an NCI SPECS grant (UO1-CA 114778), and by the Foundation for NIH, through a gift from the Richard A. Lauderbaugh Memorial Fund. This study was conducted under the auspices of the Lymphoma/Leukemia Molecular Profiling Project (LLMPP). R.S. is supported by the Dr Mildred Scheel Stiftung für Krebsforschung (Deutsche Krebshilfe). P.R. was an HHMI-NIH Research Scholar. This study used the high-performance computational capabilities of the Biowulf Linux cluster at the National Institutes of Health, Bethesda, Maryland (http://biowulf.nih.gov). We thank D. Staudt for discussions, K. Meyer for help with the GEO submission, and X. Li for IRAK1 plasmids. We are grateful to B. Tran and the Center for Cancer Research Sequencing Facility for implementation of next generation RNA sequencing.

References

1. Lenz G, et al. Stromal gene signatures in large-B-cell lymphomas. N. Engl. J. Med. 2008; 359:2313–2323. [PubMed: 19038878]
2. Iwasaki A, Medzhitov R. Regulation of adaptive immunity by the innate immune system. Science. 2010; 327:291–295. [PubMed: 20075244]
3. Ishii KJ, Akira S. Innate immune recognition of, and regulation by, DNA. Trends Immunol. 2006; 27:525–532. [PubMed: 16979939]
4. Lenz G, Staudt LM. Aggressive lymphomas. N. Engl. J. Med. 2010; 362:1417–1429. [PubMed: 20393178]
5. Lenz G, et al. Oncogenic CARD11 mutations in human diffuse large B cell lymphoma. Science. 2008; 319:1676–1679. [PubMed: 18323416]
6. Compagno M, et al. Mutations of multiple genes cause deregulation of NF-κB in diffuse large B-cell lymphoma. Nature. 2009; 459:717–721. [PubMed: 19412164]
7. Kato M, et al. Frequent inactivation of A20 in B-cell lymphomas. Nature. 2009; 459:712–716. [PubMed: 19412163]
8. Davis RE, et al. Chronic active B-cell-receptor signalling in diffuse large B-cell lymphoma. Nature. 2010; 463:88–92. [PubMed: 20054396]
9. Lam LT, et al. Cooperative signaling through the signal transducer and activator of transcription 3 and nuclear factor-κB pathways in subtypes of diffuse large B-cell lymphoma. Blood. 2008; 111:3701–3713. [PubMed: 18160665]
10. Ding BB, et al. Constitutively activated STAT3 promotes cell proliferation and survival in the activated B-cell subtype of diffuse large B-cell lymphomas. Blood. 2008; 111:1515–1523. [PubMed: 17951530]
11. Lin SC, Lo YC, Wu H. Helical assembly in the My D88–IRAK4–IRAK2 complex in TLR/IL-1R signalling. Nature. 2010; 465:885–890. [PubMed: 20485341]
12. Xu Y, et al. Structural basis for signal transduction by the Toll/interleukin-1 receptor domains. Nature. 2000; 408:111–115. [PubMed: 11081518]
13. Li C, Zienkiewicz J, Hawiger J. Interactive sites in the MyD88 Toll/interleukin (IL) 1 receptor domain responsible for coupling to the IL1β signaling pathway. J. Biol. Chem. 2005; 280:26152–26159. [PubMed: 15849357]
14. Lenz G, et al. Molecular subtypes of diffuse large B-cell lymphoma arise by distinct genetic pathways. Proc. Natl Acad. Sci. USA. 2008; 105:13520–13525. [PubMed: 18765795]

15. Jiang Z, et al. Details of Toll-like receptor:adapter interaction revealed by germ-line mutagenesis. Proc. Natl Acad. Sci. USA. 2006; 103:10961–10966. [PubMed: 16832055]
16. Yamin TT, Miller DK. The interleukin-1 receptor-associated kinase is degraded by proteasomes following its phosphorylation. J. Biol. Chem. 1997; 272:21540–21547. [PubMed: 9261174]
17. Powers JP, et al. Discovery and initial SAR of inhibitors of interleukin-1 receptor-associated kinase-4. Bioorg. Med. Chem. Lett. 2006; 16:2842–2845. [PubMed: 16563752]
18. Shaffer AL, et al. A library of gene expression signatures to illuminate normal and pathological lymphoid biology. Immunol. Rev. 2006; 210:67–85. [PubMed: 16623765]
19. Davis RE, Brown KD, Siebenlist U, Staudt LM. Constitutive nuclear factor κB activity is required for survival of activated B cell-like diffuse large B cell lymphoma cells. J. Exp. Med. 2001; 194:1861–1874. [PubMed: 11748286]
20. Dierlamm J, et al. Characteristic pattern of chromosomal gains and losses in marginal zone B cell lymphoma detected by comparative genomic hybridization. Leukemia. 1997; 11:747–758. [PubMed: 9180302]
21. Novak U, et al. The NF-κB negative regulator TNFAIP3 (A20) is inactivated by somatic mutations and genomic deletions in marginal zone B-cell lymphomas. Blood. 2009; 113:4918–4921. [PubMed: 19258598]
22. Staudt LM. Oncogenic activation of NF-κB. Cold Spring Harb. Perspect. Biol. 2010; 2:a000109. [PubMed: 20516126]
23. Milhollen MA, et al. MLN4924, a NEDD8-activating enzyme inhibitor, is active in diffuse large B-cell lymphoma models: rationale for treatment of NF-κB-dependent lymphoma. Blood. 2010; 116:1515–1523. [PubMed: 20525923]
24. Lam LT, et al. Small molecule inhibitors of IκB kinase are selectively toxic for subgroups of diffuse large B-cell lymphoma defined by gene expression profiling. Clin. Cancer Res. 2005; 11:28–40. [PubMed: 15671525]
25. Ngo VN, et al. A loss-of-function RNA interference screen for molecular targets in cancer. Nature. 2006; 441:106–110. [PubMed: 16572121]

References

26. Schmidlin H, Diehl SA, Blom B. New insights into the regulation of human B-cell differentiation. Trends Immunol. 2009; 30:277–285. [PubMed: 19447676]
27. Schmitz R, et al. *TNFAIP3* (A20) is a tumor suppressor gene in Hodgkin lymphoma and primary mediastinal B cell lymphoma. J. Exp. Med. 2009; 206:981–989. [PubMed: 19380639]

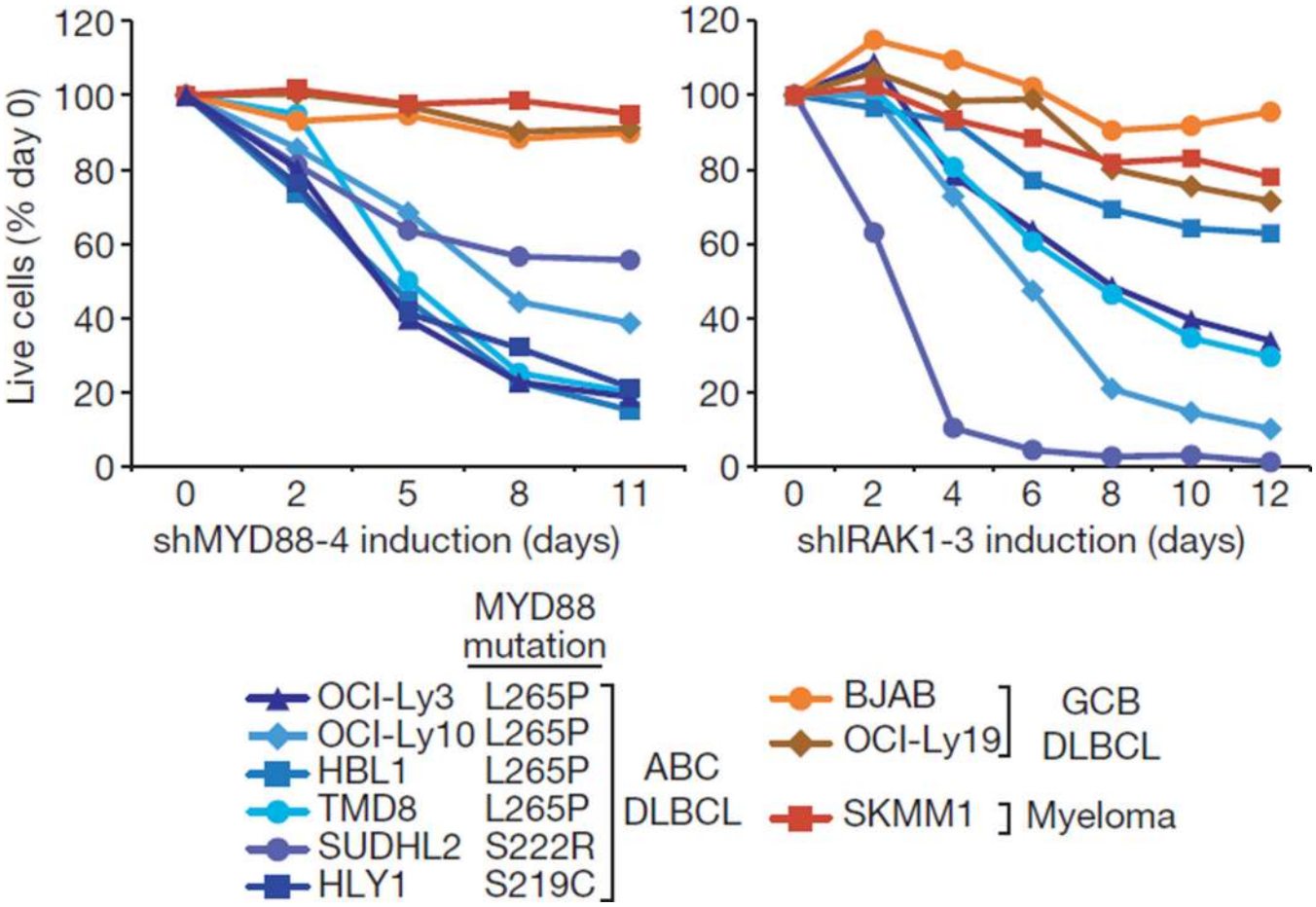

Figure 1. MYD88 is required for survival of ABCDLBCL cells

MYD88 and *IRAK1* shRNAs have selective toxicity for ABC DLBCL lines. Shown is the fraction of GFP^+, shRNA-expressing cells relative to the GFP^-, shRNA-negative fraction at the indicated times, normalized to the day 0 values.

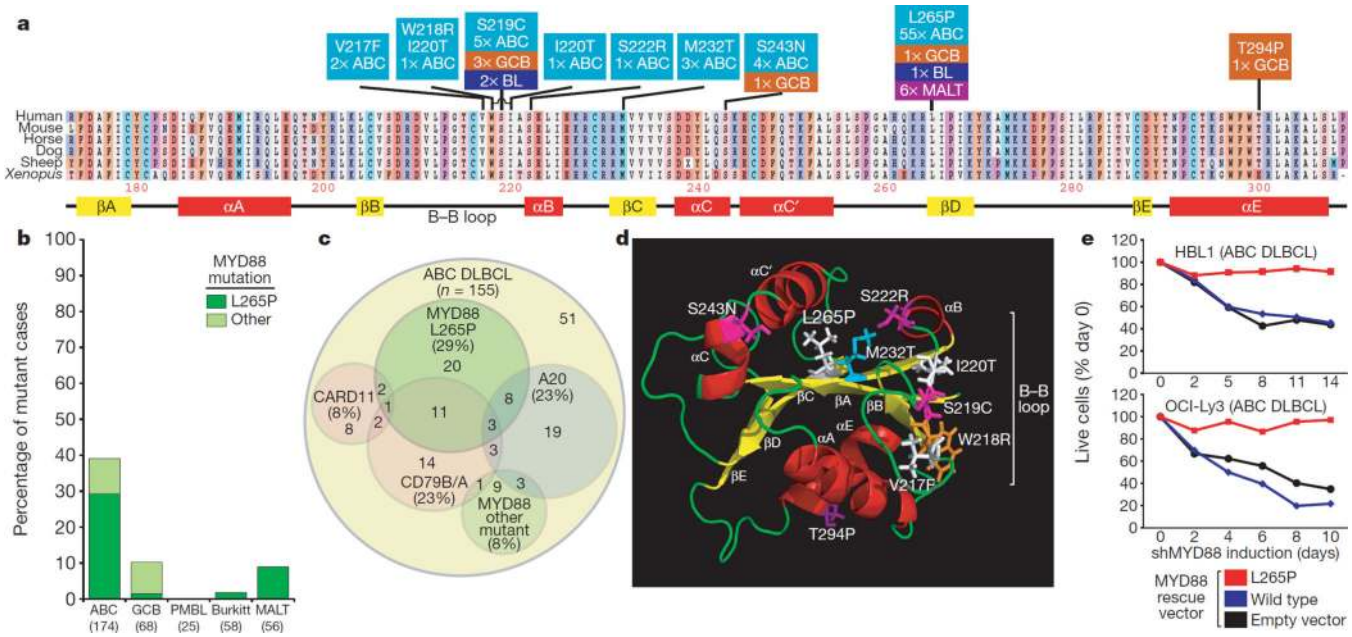

Figure 2. MYD88 mutations in human lymphomas

a, *MYD88* missense mutations in lymphoma biopsies and cell line models of ABC DLBCL (light blue), GCB DLBCL (orange), MALT lymphoma (purple) and Burkitt's lymphoma (BL; dark blue). Amino acid positions are shown according to protein accession NP_002459. **b**, Frequencies of *MYD88* mutations in biopsy samples from different lymphoma subtypes. **c**, Overlap of *MYD88* mutations with other recurrent genetic alterations in ABC DLBCL tumour specimens. Genetic subsets were defined by somatic mutations and, in the case of the A20 subset, by homozygous deletion or epigenetic silencing. **d**, Location of *MYD88* mutations in the three-dimensional structure of the MYD88 TIR domain. **e**, Dependence of ABC DLBCLs on *MYD88* L265P. A 3′-UTR-directed *MYD88* shRNA was inducibly expressed in the indicated ABC DLBCL lines, which were stably transduced with rescue vectors expressing wild-type or L265P *MYD88* coding regions, or with an empty vector. Shown is the fraction of viable shRNA-expressing cells relative to the shRNA-negative fraction, normalized to day 0 values.

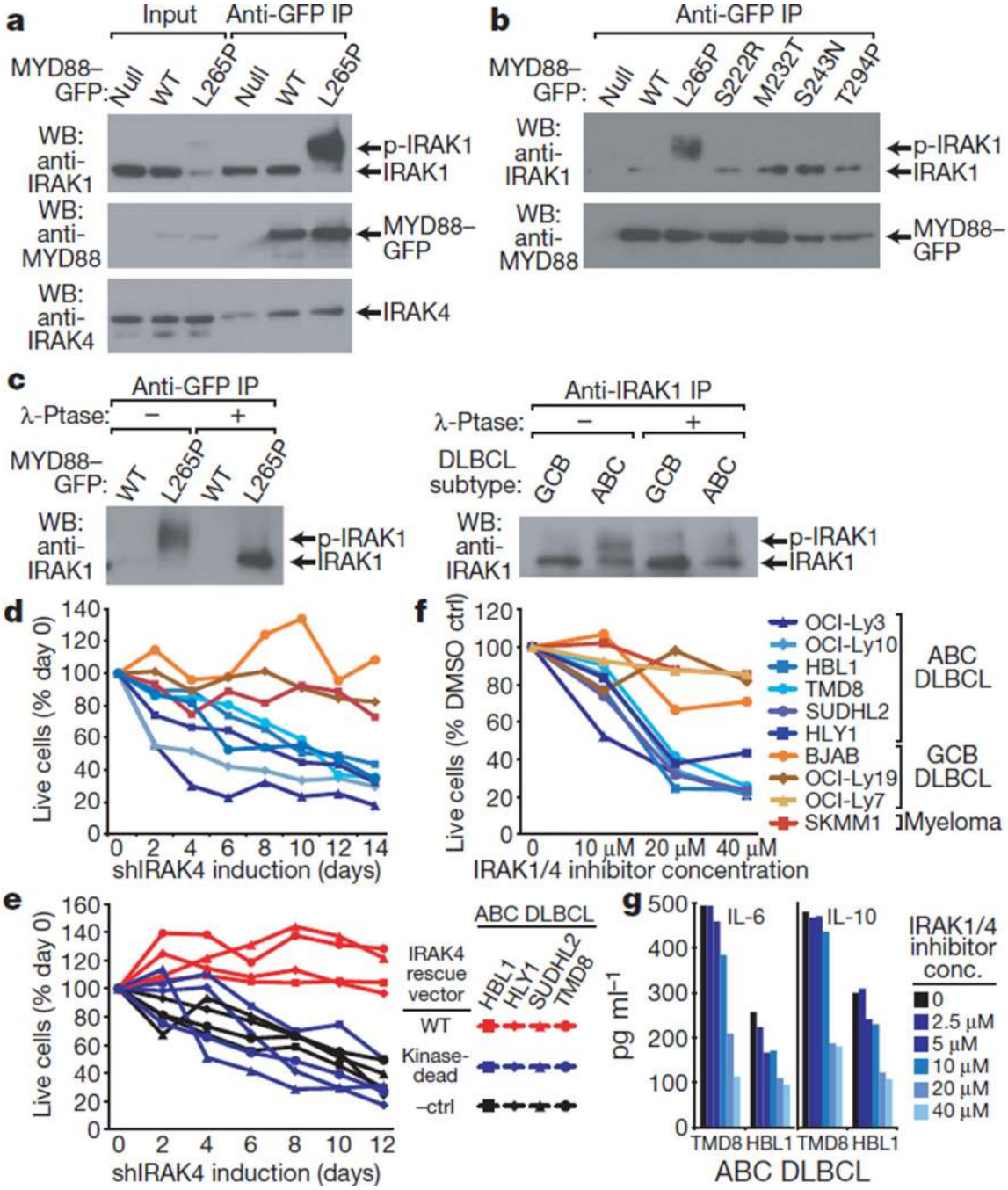

Figure 3. MYD88 mutations are gain-of-function

a, An altered IRAK1 isoform associated with MYD88 L265P. The GCB DLBCL line BJAB was transduced with GFP-tagged wild-type (WT) or L265P MYD88, or with an empty vector (null). Anti-GFP immunoprecipitates (IP) and input lysates were examined by immunoblotting for IRAK1, IRAK4 and MYD88. **b**, Preferential association of an altered IRAK1 isoform with MYD88 L265P. BJAB cells were transduced with the indicated GFP-tagged MYD88 isoforms and examined as in **a**. **c**,MYD88 L265P associates with phosphorylated IRAK1. Top panel: BJAB cells were transduced with the indicated GFP-

tagged MYD88 isoforms. Anti-GFP immunoprecipitates were treated with λ-phosphatase as indicated and examined by immunoblotting for IRAK1 or MYD88. Bottom panel: anti-IRAK1 immunoprecipitates from HBL1 (ABC) or BJAB (GCB) cells were treated with λ-phosphatase as indicated and examined by immunoblotting for IRAK1. **d**, Toxicity of *IRAK4* shRNAs for ABC DLBCLs. The indicated lines were transduced with retroviruses expressing *IRAK4* shRNA and the relative number of shRNA$^+$ cells is plotted versus time after shRNA induction, normalized to day 0. Data are representative of experiments with three different *IRAK4* shRNAs. **e**, IRAK4 kinase activity is required for ABC DLBCL survival. The indicated ABC DLBCL lines were transduced with retroviruses expressing wild-type or kinase-dead IRAK4 isoforms, or with an empty vector (−ctrl). The survival of cells after induction of an *IRAK4* shRNA is shown. **f**, A small-molecule IRAK1/4 kinase inhibitor is selectively lethal for ABC DLBCLs. Viability of the indicated lines was measured after treatment for 3 days with various inhibitor concentrations and normalized to DMSO-treated cells. **g**, IRAK4 kinase activity regulates IL-6 and IL-10 secretion. The indicated cytokines were measured in the supernatant of ABC DLBCL lines after treatment for 24 h with various concentrations of the IRAK1/4 inhibitor.

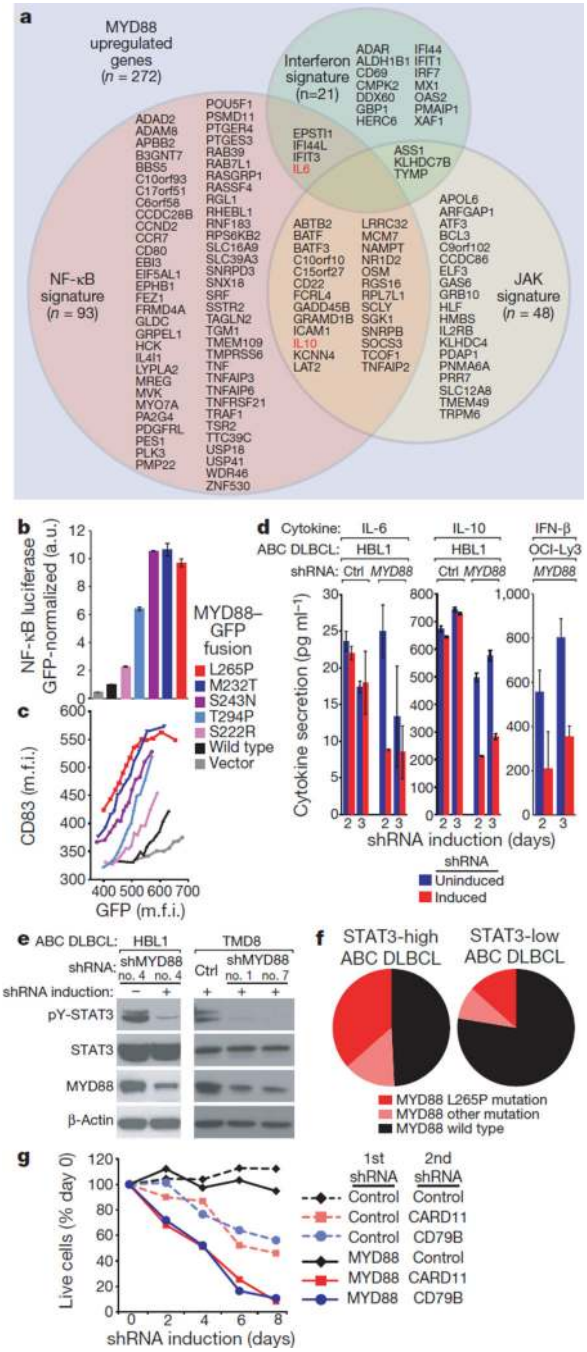

Figure 4. MYD88mutants activate NF-κB and cytokine signalling

a, Venn diagram of genes affected by MYD88 knockdown in the HBL1 ABC DLBCL line, grouped according to membership in gene expression signatures. **b**, MYD88 mutants constitutively activate NF-κB. BJAB cells co-expressing the indicated MYD88–GFP mutants and a NF-κB-driven luciferase reporter construct were assayed for luciferase activity, which was normalized to the expression levels of each MYD88–GFP isoform. a.u., arbitrary units. **c**, Correlation of MYD88 protein levels with CD83 expression. BJAB cells bearing GFP-tagged MYD88 isoforms were assessed for CD83 and GFP expression. Cells

were assigned to equally sized bins based on their GFP levels, and the mean fluorescence intensity (m.f.i.) of CD83 in each bin was plotted. **d**, MYD88 knockdown decreases cytokine secretion in ABC DLBCL. *MYD88* or control (ctrl) shRNAs were induced in ABC DLBCL lines, and the indicated cytokines were measured in the supernatant over time. **e**, STAT3 phosphorylation in ABC DLBCL depends on MYD88. *MYD88* or control (ctrl) shRNAs were induced in ABC DLBCL lines, and cells were assessed by immunoblotting for phosphorylated STAT3 (pY-STAT3), total STAT3, MYD88 and β-actin. **f**, Preferential association of MYD88 mutant isoforms with the STAT3-high subgroup of ABC DLBCL tumours. See text for details. **g**, MYD88 and B-cell-receptor signalling pathways cooperate to maintain ABC DLBCL survival. OCI-Ly10 ABC DLBCL cells were first transduced with retroviruses expressing *MYD88* or control shRNAs and then infected with retroviruses expressing *CD79A, CARD11*, or control shRNAs along with GFP. The relative viability of GFP^+ cells is plotted, normalized to day 0 values. All error bars are s.e.m. ($n = 3$).